KONA Powder and Particle Journal

KONA Powder and Particle Journal No. 43 (2026) 224–237/https://doi.org/10.14356/kona.2026001 Original Research Paper

Effect of Temperature on Aluminium Powder Flowability and Spreadability †

Mozhdeh Mehrabi [1], Fatemeh Ali Akbar Talebi [1], Nathan Berry [2], Sorush Khajepor [2], Sina Haeri [2], Jabbar Gardy [3], Joseph Oluleke [4], Andrew Bayly [1] and Ali Hassanpour [1]*

[1] *School of Chemical and Process Engineering, University of Leeds, UK*
[2] *School of Engineering, University of Edinburgh, UK*
[3] *Cormica Limited, UK*
[4] *Carpenter Additive, UK*

In powder-based Additive Manufacturing (AM) the precise control of process parameters plays a significant role in the quality and efficiency of the printing process. Among these, the effect of temperature has received less attention in the literature, although it is a significant factor that influences the inter-particle forces and, consequently the powder flow and spreading behaviour of powders. In selective laser sintering (SLS) or selective laser melting (SLM), pre-heating the chamber and powder bed is a required step prior to sintering, hence, the temperature can significantly influence the layer adhesion and spread quality. In this context, the present study explores the effect of elevated temperature on the flow and spreading behaviours of AlSi10Mg powders. The flow properties of two different grades of aluminium alloy powders are characterised using the Carney and Hall flow tests, angle of repose and shear test techniques at different temperatures and correlated with the spreading behaviour at elevated temperatures, measured using the spreading rig with a heated bed developed at the University of Leeds. This study revealed that at elevated temperatures the spreadability of AlSi10Mg powders worsens because of changes in interparticle forces and particle surface interactions.

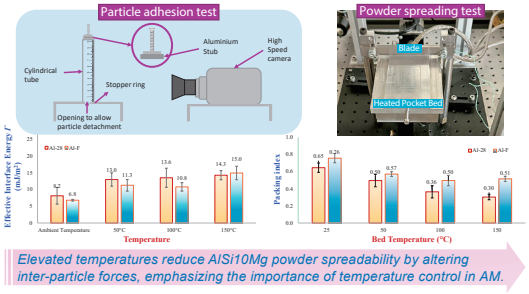

Keywords: Additive Manufacturing, spreadability, flowability, temperature, AlSi10Mg

1. Introduction

Additive Manufacturing (AM) is an innovative process that is beginning to reshape the manufacturing industry. Although AM has great potential for enabling creativity and improving efficiency, there are concerns regarding the consistency of part properties manufactured by AM, as the influences of feed properties and process conditions are not yet fully understood (Dowling et al., 2020; LeBrun, 2024; Venturi and Taylor, 2023).

Powder Bed Fusion (PBF) is one of the most well-known AM processes, as outlined in ISO/ASTM 52900 (ASTM, 2015), and relies on powder as its foundation material. The PBF process requires the precise delivery of a thin layer of powder from a storage and feed system to the fusion platform. Subsequently, the powder undergoes selective fusion in accordance with a pre-established CAD file. This iterative process continues until the desired shape of the manufactured component is obtained. One of the main concerns regarding PBF processes, such as selective laser sintering (SLS), selective laser melting (SLM), and electron beam melting (EBM) is achieving a uniform powder layer before fusion (Gibson et al., 2021; Oropeza et al., 2022). In these processes, maintaining a consistent layer thickness at each stage is essential, because it greatly affects the precision and quality of the final product (Mindt et al., 2016; Snow et al., 2019; Vock et al., 2019).

Several factors can affect the spreading behaviour of powder and the spread layer characteristics (e.g. powder bed density distribution) such as physical and chemical properties of feedstock (Haydari et al., 2024; He et al., 2021; Mehrabi et al., 2023; Strondl et al., 2015), the spreading mechanism (Fouda and Bayly, 2020; Mehrabi et al., 2023; Reijonen et al., 2023), and the environmental conditions of storage (Cordova et al., 2017; Grubbs et al., 2022). In the past two decades, numerous researchers have attempted to propose correlations between powder properties, specifically the physical properties of powder and bulk flow behaviour, and their relationship with spreadability (Balbaa et al., 2021; He et al., 2021; Jacob et al., 2018; Mehrabi et al., 2023; Strondl et al., 2015; Touzé et al., 2020). However, some crucial factors, such as the effect of elevating the temperature of the build plate, which is a key feature of PBF processes, on the spreadability of powder have not been thoroughly considered. Using a pre-heating

† Received 14 August 2024; Accepted 8 October 2024
J-STAGE Advance published online 27 December 2024
* Corresponding author: Ali Hassanpour;
Add: LS2 9JT Leeds, UK
E-mail: a.hassanpour@leeds.ac.uk
TEL: +44(0)113 343 2405

stage in the PBF process often has several advantages, including the reduction of thermal stress related issues that occur during fabrication in SLM and SLS processes, and subsequent minimisation of detrimental residual stresses in the final component (Li et al., 2018). Nevertheless, a pre-heated powder bed is an environmental process condition that could significantly affect the powder behaviour and play an important role in the flowability and spreadability of the powders (Liu et al., 2015; Papazoglou et al., 2022).

Some studies have focused on the effect of temperature on powder flowability. Zhang and Liu (2023) used a heated rotating drum along with a high-speed camera to record nylon and stainless steel powders avalanche processes at elevated temperatures, for the characterisation of powder flowability and spreadability (Zhang and Liu, 2023). Their findings indicated that nylon powder begins to soften and agglomerate at 160 °C, leading to deterioration of its flowability. In contrast, the impact of temperature on the flowability of the steel powder was less pronounced. Recently, Ajabshir et al. (2024) investigated the effect of temperature (25 °C and 110 °C) and spreading speed (3 mm/s and 30 mm/s) on the spreading behaviour of polyamide powder in the AM process using both the Discrete Element Method (DEM) and experimental characterisation (Ajabshir et al., 2024; Zinatlou Ajabshir et al., 2024). The results indicate that the packing fraction of these polymer powders decreases with increasing the temperature or spreading speed, suggesting a less uniform spread of the powder bed at higher temperatures. Although the effect of elevated temperature on spreading has been numerically and experimentally studied in their research, to the best of our knowledge no such experimental work has been reported on any metal powder.

Aluminium alloys have received increasing attention in SLM due to their suitability for structural applications in the automotive and aerospace industries (Chen et al., 2018). Literature has shown that components made from aluminium alloy including AlSi10Mg and AlSi12 exhibit high strength, toughness, and significant strain hardening ability (Chen et al., 2018; Prashanth et al., 2017; Suryawanshi et al., 2016). However, AlSi10Mg is highly sensitive to water and oxygen absorption, and both process parameters and environmental conditions can significantly affect the flow and spreading behaviour of the powder (Cordova et al., 2017; Weiss et al., 2022). The influence of environmental conditions such as humidity and temperature on the quality of AM parts manufactured using AlSi10Mg powder has been reported in the literature. Riener et al. (2021) explored the impact of storage conditions on AlSi10Mg powder and its subsequent effects on the final parts manufactured via the Laser Powder Bed Fusion (LPBF) process. Their findings indicate that when the powder is stored in humid conditions, the resulting printed parts exhibit lower density and mechanical strength. However, this degradation can be mitigated by subjecting the powder to drying in a vacuum oven (Riener et al., 2021). In another study, it was reported that the strength of AlSi10Mg manufactured parts decreased significantly with increasing build platform temperature from 35 °C to 200 °C (Santos Macías et al., 2020).

Despite the reported connection between the environmental parameters and the mechanical properties of the final component made of AlSi10Mg powder, less attention has been given to how the process parameters of SLM (specifically, the pre-heating of the bed plate) would affect the spreading behaviour of the powder. To date, no work has examined the effect of a pre-heated chamber on the spreading behaviour of ALSi10Mg powder (Avrampos and Vosniakos, 2022). Therefore, the aim of this study is to investigate the effect of temperature on the particle interactions, flowability and spreading behaviour of aluminium powders. Various flowability techniques have been employed to assess the powder flow behaviour at ambient and elevated temperatures. Furthermore, the powder flow characteristics are compared with the powder spreading behaviour under ambient and elevated temperatures.

2. Materials and methodology

2.1 Materials

Two different batches of Electrode Inert Gas Atomisation (EIGA) produced AlSi10Mg powders, namely Al-F (**Fig. 1(a), (b)**) and Al-28 (**Fig. 1(c), (d)**), supplied by Carpenter Additive, were investigated to compare their flow, and spreading behaviour at normal and elevated temperatures. The scanning electron microscopy (SEM) images shown in **Fig. 1** demonstrate that both powders exhibit comparable shapes which are spheroidal in nature, with the presence of satellites on their surfaces.

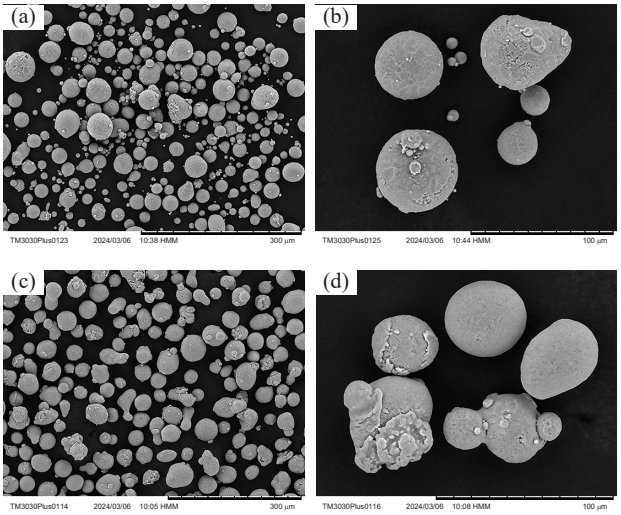

Fig. 1 SEM images of **(a)**, **(b)** Al-F and **(c)**, **(d)** Al-28 powders. Images are produced by the authors.

2.2 Experimental procedures

To investigate the physical and chemical properties of powders, various techniques were employed to analyse factors such as size distribution, shape, chemical composition, and moisture content.

2.2.1 Particle size distribution

The size distribution of powders plays a critical role in determining their bulk properties and behaviours, such as flowability, packing density, and spreading behaviour. The particle size distribution of the powders was measured by laser diffraction using the Mastersizer 3000 Particle Size Analyzer (Malvern Panalytical, UK).

2.2.2 Particle shape characterisation

Since particle shape plays an important role in additive manufacturing, it is important to accurately analyse particle shape characteristics. The Morphologi G3 (Malvern Panalytical, UK) was used for this purpose. This advanced tool, based on automated microscopy and image analysis software, provided detailed measurements such as aspect ratio (a function of the smallest Feret's diameter and the largest orthogonal diameter), circularity (closeness to a perfect circle), convexity (edge roughness), and solidity (overall concavity) for both powder samples.

2.2.3 Moisture characterisation

As mentioned in literature, aluminium alloys have a higher tendency to absorb moisture than steel or titanium powders (Cordova et al., 2017; Weiss et al., 2022). This increased moisture absorption can lead to oxidation and reduced performance in additive manufacturing. To evaluate this characteristic, the moisture absorption tendency of both powders was analysed using a saturated aqueous solution method, as outlined by Greenspan (1977). This technique involves placing the powders in a controlled environment with known relative humidity, which is maintained using a saturated salt solution. The solution creates a stable humidity level, allowing for the precise measurements of the amount of moisture the powders absorb over time. By weighing the powders before and after exposure, the weight fraction of absorbed moisture can be calculated. This method is widely used due to its reliability in simulating real-world moisture conditions and its ability to provide insight into how powders may behave during storage or processing.

2.2.4 Chemical composition

The chemical composition of both powders was analysed using Backscattered Electron Imaging (BSE) Scanning Electron Microscopy (SEM) coupled with Energy Dispersive X-ray Spectroscopy (EDS) to identify the elements present in each sample. BSE imaging provides visual information based on variations in grey-scale intensity, which correspond to differences in atomic numbers across chemical phases. High-energy backscattered electrons reflected from the sample surface produce these intensity variations, with the number of backscattered electrons directly correlating to the atomic number of the elements present. EDS complements BSE by providing identification of the elemental composition within the sample.

2.2.5 Flowability characterisation

Several techniques commonly used in the powder industry, particularly in AM, have been employed to characterise the flowability of the powders under ambient conditions, with an average relative humidity of 40–50 % and a temperature range of 20–22 °C, as described below (Mehrabi, 2021; Mehrabi et al., 2023).

2.2.5.1 Angle of Repose (AOR)

The Angle of Repose (AOR) method is a simple technique for evaluating powder flow characteristics (Geldart et al., 2009), which has been cautiously implemented for AM powders. For the AOR tests in this project, 100 g of powder was used, and the tests were repeated until minimum variation in iterations was achieved.

2.2.5.2 Bulk and tapped density measurements

The determination of bulk and tapped densities, which involves measuring the powder density in both loose and compacted states, has also been applied to AM powders. In this method, the Hausner ratio (HR), i.e., the ratio of tapped to bulk density (Hausner, 1967), and Carr index (CI), i.e., the ratio of the difference between the tapped and bulk densities to the tapped density (Carr, 1965), are calculated and can be used to evaluate flow behaviour of powders. In this work, the JV 2000 tapped density tester (Copley Sci., UK) was used. The cylinder containing 100 g of powder was tapped for 30 min until the volume stabilised. The initial and final volumes of both samples were recorded to determine their bulk and tapped densities, as well as the Carr index and the Hausner ratio.

2.2.5.3 Flowrate test

It is a common and relatively simple method to characterise the flow behaviour of metal powders based on the time needed to release a specific amount of powder through an orifice of known size. The flowrate test is simple and can be used for AM powders (ASTM B213-20) (ASTM, 2020). In this test, 50 g of powder was deposited through 2.5 mm and 5 mm orifice openings, which are known as the Hall and Carney funnel flows, respectively.

2.2.5.4 Powder Rheology

The FT4 Powder Rheometer® (Micromeritics Instrument Corporation) is a standardised instrument for measuring the flow resistance of powders under dynamic conditions (Freeman, 2007). It has become increasingly popular for characterising powder flow for AM applications (Clayton et al., 2015; Murtaza et al., 2023). In this study, the required energy to displace powder in a confined

condition, per unit mass of powder, known as Normalised Basic Flowability Energy (NBFE), as well as the energy required for powder movement in an unconfined condition (Specific Energy, SE) were measured.

2.2.5.5 Shear testing—Schulze ring shear tester®

This technique is a universally recognised measurement method used to assess flowability under moderate or high stress conditions. It offers excellent reproducibility and ensures consistent results across experiments (Freeman, 2007). Despite not aligning perfectly with the conditions of AM application, where powder only goes through low stress conditions during spreading, the method is widely regarded as reliable and is well-established in both research and industry (Ganesan et al., 2008; Rüther et al., 2023). The flowability of powders can be assessed by using the flow function coefficient (ff_c), which is represented by the ratio of the Major Principal Stress (σ_1) to the Unconfined Yield Strength (σ_c) at a specified normal load from Mohr's circles (**Eqn. (1)**) (Jenike, 1987).

$$ff_c = \frac{Major\ Principal\ Stress\ (\sigma_1)}{Unconfined\ Yield\ Strength\ (\sigma_c)} \quad (1)$$

As illustrated in **Fig. 2**, from Mohr's circles, various important parameters can be extracted to investigate the flow properties of the powders. The internal angle of friction (φ_{lin}), defined by the line running through the pre-shear points, demonstrates the powder's ability to withstand shear stress. The effective internal angle of friction (φ_e), which represents the friction between the sliding layers of the powder, is obtained from the tangent to the largest Mohr circle passing through the origin.

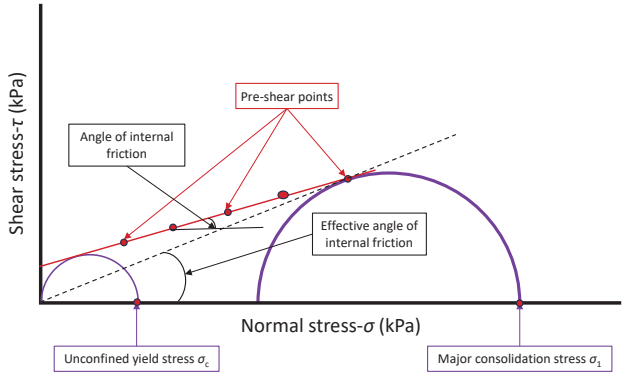

Fig. 2 Graphical description of flowability parameters derived from Mohr's circle.

3. Results and discussions

3.1 Size distribution

The particle size distribution measured by laser diffraction on the dry dispersed powders shows that the Al-F powder has a slightly wider size distribution compared to the Al-28 powder (**Fig. 3**).

3.2 Shape characterisation

The shape characteristics of the powders are summarised in **Table 1**. The aspect ratio and circularity values of the Al-28 powder were found to be lower than those of the Al-F powder, indicating that the Al-28 particles are less spherical or have more satellites than the Al-F powder.

3.3 Chemical composition

Powder chemical compositions were determined using Energy Dispersive X-ray Spectroscopy (EDS). The elemental compositions of the samples are listed in **Table 2**. An important observation from the EDS results was that

Table 1 Shape characterisation of the powders.

	Aspect ratio (-)	Circularity (-)	Convexity (-)	Solidity (-)
Al-28	0.87	0.95	0.99	0.98
Al-F	0.96	0.98	0.99	0.99

Table 2 The elemental compositions of samples Al-28 and Al-F determined by EDS.

Element	Al-28 (wt.%)	Al-F (wt.%)
Al	86.44	86.61
Si	10.74	11.37
Mg	0.45	0.58
O	2.06	1.03
Ag	0.20	0.21
Fe	0.11	0.20
Total	100	100

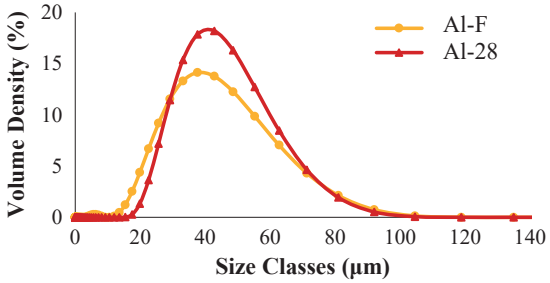

	D_{10} (µm)	D_{50} (µm)	D_{90} (µm)
Al-28	27.3	40.9	61.8
Al-F	22.1	38.2	65.9

Fig. 3 The volume-based particle size distribution of both powders.

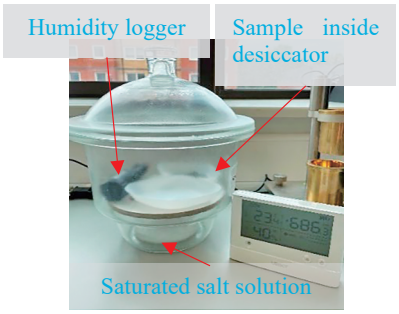

	Moisture content (wt.%)
Al-28	0.039 ± 0.009
Al-F	0.025 ± 0.004

Fig. 4 Moisture characterisation using saturated salt solution. The image is an original work by the author.

Table 3 Comparison of different flowability tests for both powders at ambient temperature.

	AOR (°)	HR	CI (%)	Hall flowrate (s/50 g)	Carney flowrate (s/50 g)	SE (mJ/g)	NBFE (mJ/g)	Scale of flowability
Al-28	27.4 ± 0.8	1.14	12.14	71 ± 0.16	14 ± 0.81	3.21 ± 0.29	7.37 ± 0.43	Free flow
Al-F	28.1 ± 0.3	1.09	7.94	65 ± 0.81	13 ± 0.02	1.59 ± 0.03	5.35 ± 0.41	Free flow

the oxygen content of the Al-28 powder was higher than that of the Al-F powder.

3.4 Moisture characterisation

To analyse the moisture absorption behaviour of the powders, 10 g of each powder was placed in a controlled and sealed desiccator with ~ 75 % relative humidity generated by a saturated solution of sodium chloride. After 24 hours, the weight gain was measured (**Fig. 4**). Each sample was evaluated thrice to assess the degree of repeatability. The results indicate that Al-28 has a higher tendency to absorb moisture, likely due to the higher Wt.% of oxygen, most probably because of an increased oxide layer that tends to absorb more moisture. This difference could be an important factor affecting the bulk behaviour of the powder at ambient temperature, and increasing the temperature could either improve or degrade the layer, which requires further attention.

3.5 Flowability measurements at ambient temperatures

The results of the flowability techniques described in **Section 2**, which included AOR, density measurement, flowrate, and powder rheology, conducted under ambient conditions (relative humidity of 40–50 % and temperature of 20–22 °C), are presented in **Table 3**.

It can be observed that, with the exception of AOR, the Al-F powder exhibits better flowability in all techniques. However, the difference between their AOR values was within the range of their standard deviation. Nevertheless, both powders are considered free flowing according to the flowability scale of all the aforementioned techniques.

The flow functions and internal angles of friction obtained from shear testing of both powders are presented in **Figs. 5** and **6**, respectively. The flow function results from

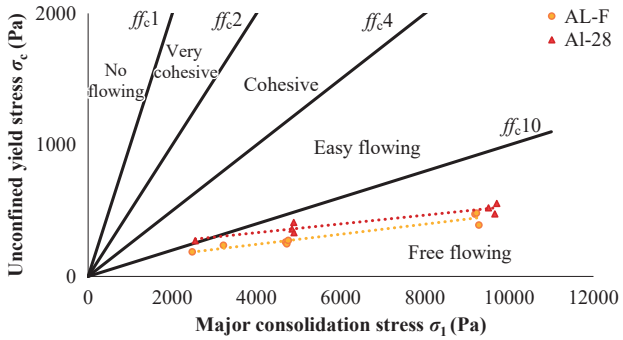

Fig. 5 The results of shear test for samples F and 28 (AlSi10Mg) at ambient temperature.

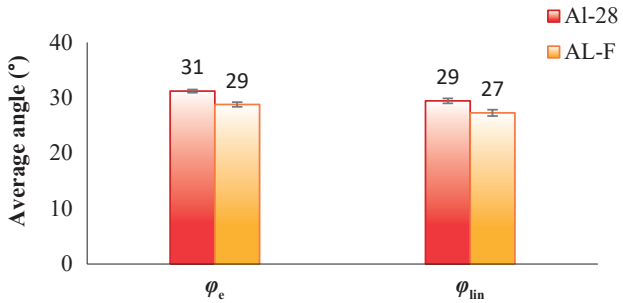

Fig. 6 Average internal angle of friction (φ_{lin}) and effective internal angle friction (φ_e) for both powders at ambient temperature.

Fig. 5 show both powders are in the free-flowing region under higher consolidation stress. At lower consolidation stress (<3 kPa), both powder flow behaviours deteriorate and get closer to the easy-flowing region, with Al-28 showing slightly poorer flowability.

Fig. 6 shows that the Al-F powder exhibits a smaller internal angle of friction, indicating less friction and better flowability, compared to Al-28. This is consistent with the differences in shape, where it is expected that particles with

a less spherical shape have a larger internal angle of friction (>30°) (Shinohara et al., 2000).

3.6 Flowability characterisation at elevated temperatures

To investigate the effect of temperature on the powder flow behaviour, three techniques were employed at elevated temperatures: AOR, shear testing, and flowrate testing. These techniques were selected based on their ease of use at elevated temperatures, availability, and ability to understand particle motion. The AOR test is used to obtain quick, preliminary results. The Anton-Paar Modular Compact Rheometer at the University of Edinburgh was used to analyse the incipient flow behaviour of the powder at higher temperatures. Hall and Carney flowrate tests were used to understand the dynamic flow behaviour, as these have been shown to have a strong correlation with the actual behaviour of powders during spreading operations (Hulme et al., 2023; Jacob et al., 2018; Liu et al., 2019; Mahamood and Akinlabi, 2018; Park et al., 2016).

3.6.1 Angle of Repose (AOR)

To characterise the effect of elevated temperature on the AOR test, both powders were placed in a vacuum oven for 30 min at different temperatures (50, 100, 150 °C). Subsequently, they were promptly removed from the oven, and the tests were conducted three times. **Fig. 7** represents the effect of temperature on the angle of repose.

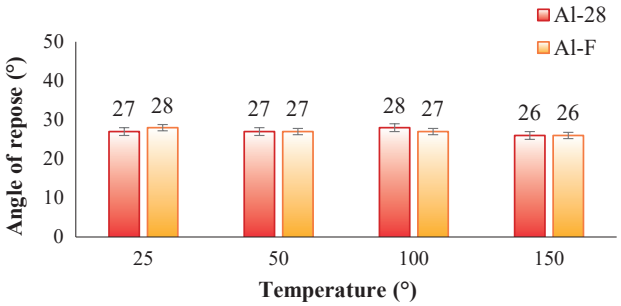

Fig. 7 Effect of temperature on the AOR of powders.

No significant impact of temperature on the angle of repose was observed, as the difference in the results lies within the range of error of the method. This technique may not be a suitable method to assess the effect of temperature on flowability, as the powder placed on the AOR rig and flowing through the funnel may lose temperature and cool down due to aeration during cone formation. It is worth noting that it was not possible to place the AOR device in an oven since it was partially made of plastic, and it had an electrical vibrator for powder discharge through a chute.

3.6.2 Anton-Paar Modular compact rheometer

Anton Paar developed a shear cell made of stainless steel (Modular Compact Rheometer, MCR 702e) enclosed by two halves of an electrical oven, allowing powder flow to be evaluated at elevated temperatures (**Fig. 8**). After filling and levelling the powder, the cell is closed and the temperature is allowed to reach the desired level. The shear test protocol can then be performed to measure the flow properties.

The results obtained for the flow function coefficient (ff_c) and internal angle of friction at room temperature were consistent with those obtained using the Schulze shear cell device. However, as the temperature increased, a corresponding increase in the variability of the pre-shear and shear data was observed. Analysis of the data presented in **Figs. 9** and **10** reveals a notable phenomenon: as the temperature increased from room temperature to 150 °C, the occurrence of stick-slip behaviour became more pronounced. The stick-slip phenomenon entails an increase in shear stress followed by a sharp drop, resulting from both material and system properties. This suggests that at elevated temperatures, the powder particles exhibit higher static friction, leading to an increase in shear stress. As a

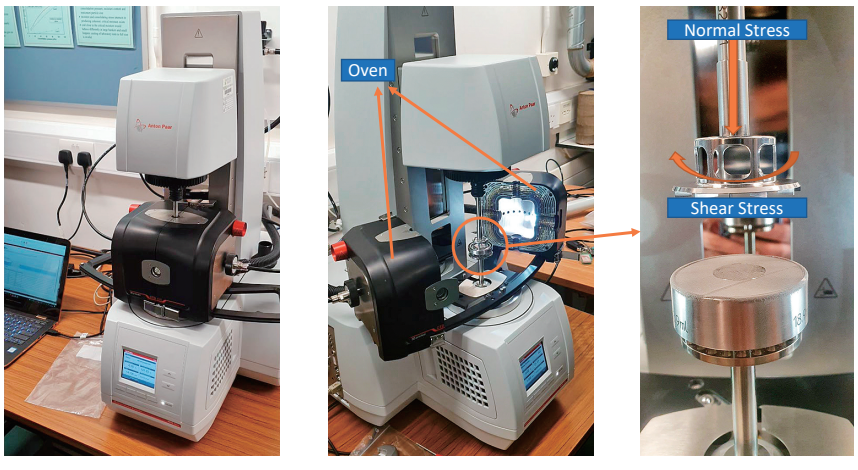

Fig. 8 Anton-Paar Modular compact rheometer at University of Edinburgh. Photographs are taken by the authors.

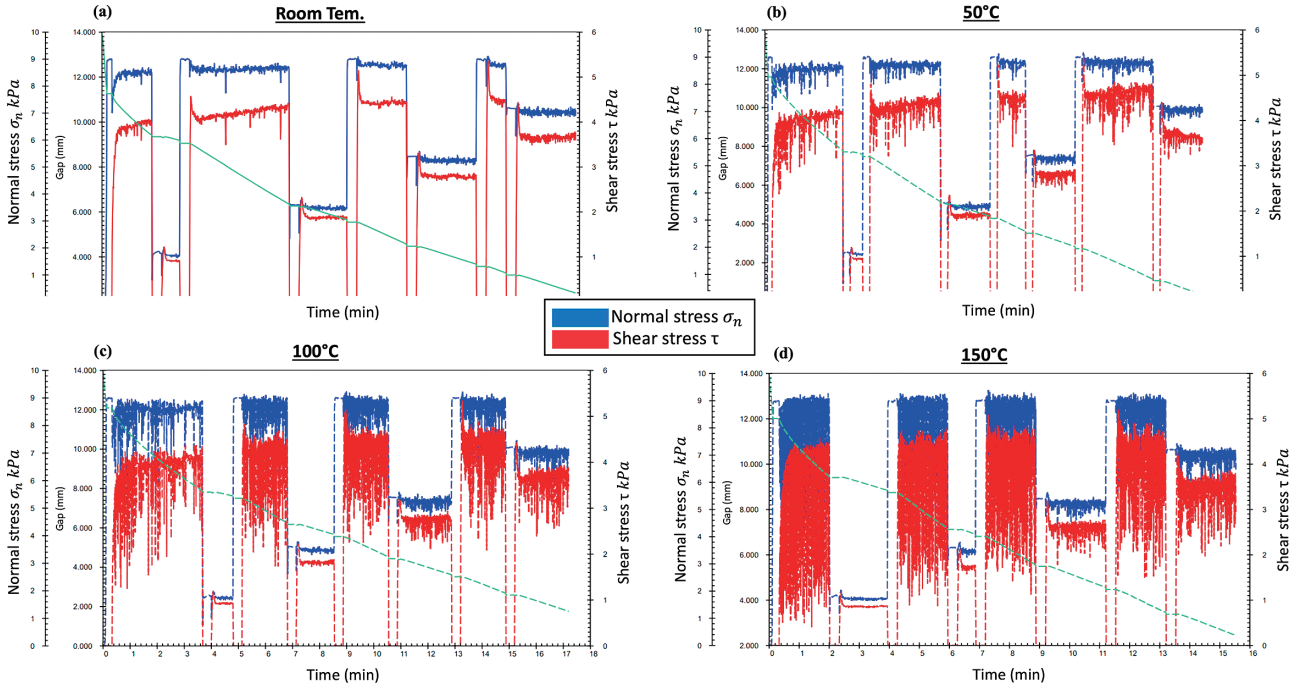

Fig. 9 Plot of shear stress vs. time for Al-F powder at **(a)** room temperature, **(b)** at 50 °C, **(c)** at 100 °C and **(d)** at 150 °C.

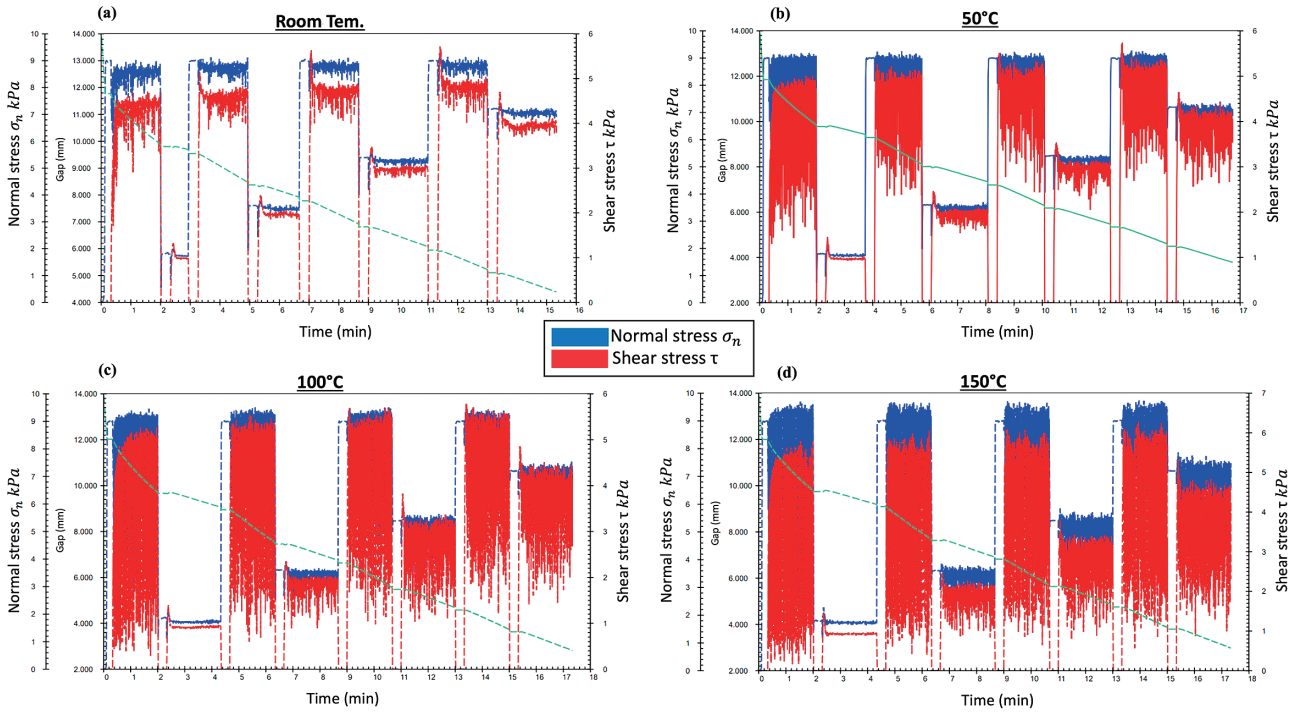

Fig. 10 Plot of shear stress vs. time for Al-28 powder at **(a)** room temperature, **(b)** at 50 °C, **(c)** at 100 °C and **(d)** at 150 °C.

result, more elastic energy can be stored in the system at the onset of the slip, leading to a stronger acceleration during the slip and a more pronounced decrease in the shear stress (Schulze, 2003). Hence, the higher levels of fluctuation observed in the data as the temperature increased suggest an increase in the sliding friction of powders with increasing temperature. However, the shear cell results, including the flow function and internal angle of friction, at elevated temperatures were inconclusive because a steady state could not be obtained (Bagga et al., 2012).

3.6.3 Flowrate test

To investigate the impact of elevated temperatures on the flowrates for both powders, a procedure similar to the AOR technique was employed. However, both the powders and the funnels (Carney and Hall) were subjected to 30 min of

heating in a vacuum oven at different temperatures (50 °C, 100 °C and 150 °C). Then, they were quickly removed from the oven, and the tests were conducted while the powders were still hot. **Figs. 11** and **12** illustrate the effect of different temperatures on the Carney and Hall flow tests, respectively.

The tests have clearly shown that the flowrate of both samples slightly decreases with increasing temperature. During the experiments, it was observed that both powders adhered to the walls of the hopper, especially at 150 °C (**Fig. 13**). This finding suggests a decrease in flowability with increasing powder temperature, which is likely due to an increase in surface energy mainly attributed to van der Waals forces. Therefore, the influence of temperature on the surface energy of powders was measured using the drop test method (Zafar et al., 2014).

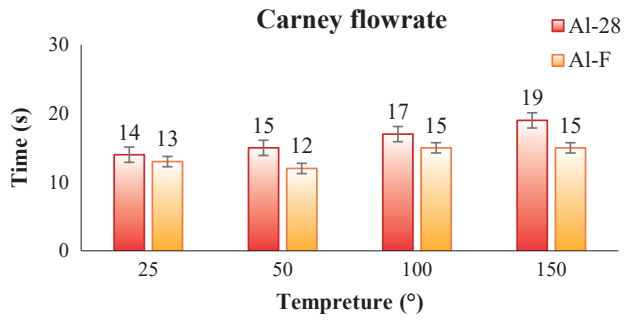

Fig. 11 Effect of temperature on the Carney flowrate for Al-F and Al-28.

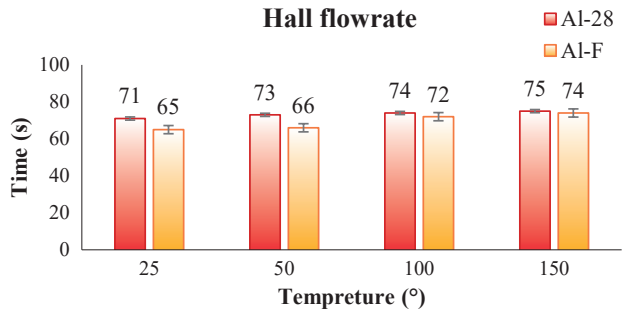

Fig. 12 Effect of temperature on the Hall flowrate for Al-F and Al-28.

3.7 Measuring particle adhesion using the drop test technique

The drop test can be used to quantify the adhesive force of particles by subjecting them to a tensile force, where the effective interfacial energy can be calculated from the balance of the detachment force derived from Newton's second law of motion and adhesive force based on the JKR theory (Zafar et al., 2014) (**Eqn. (2)**).

$$\frac{F_{det}}{F_{ad}} = \frac{\left(\frac{mv}{\Delta t}\right)}{\frac{3}{2}\pi R\Gamma} = 1 \tag{2}$$

In **Eqn. (2)**, F_{ad} is the adhesion force, Γ is the effective interfacial energy, and R is the reduced particle radius. Here, F_{det} is the detachment force, m is the mass of the particle with the critical diameter, v is the impact velocity and Δt is the stoppage time after impact.

To measure the effective interfacial energy of both powders, the experimental work was carried out using an in-house drop test rig developed at University of Leeds (**Fig. 14**).

In these experiments, both powders were deposited on aluminium stubs using the dispersion unit of the Morphologi G3, and the sizes and locations of the particles were recorded. The stubs were then dropped from a height of 10 cm, resulting in an impact velocity ranging from 1.21 m/s to 1.23 m/s against a stopper. The stoppage time

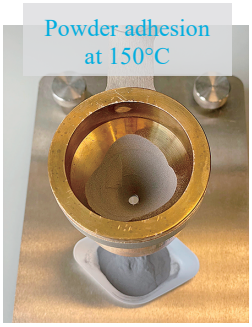

Fig. 13 Powder adhesion to the hopper at 150 °C. The photograph is taken by the authors.

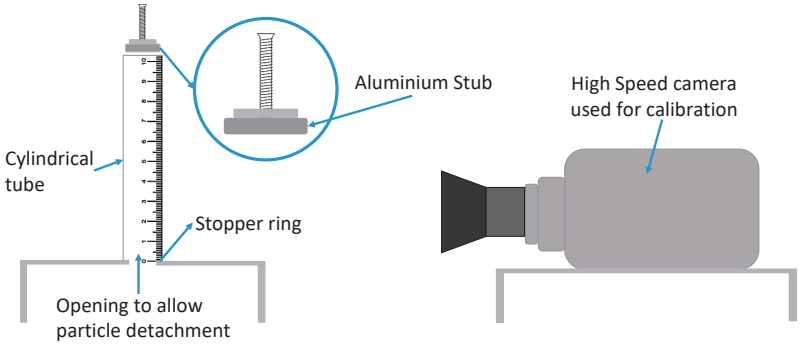

Fig. 14 The drop test rig at University of Leeds. The schematic is produced by the authors.

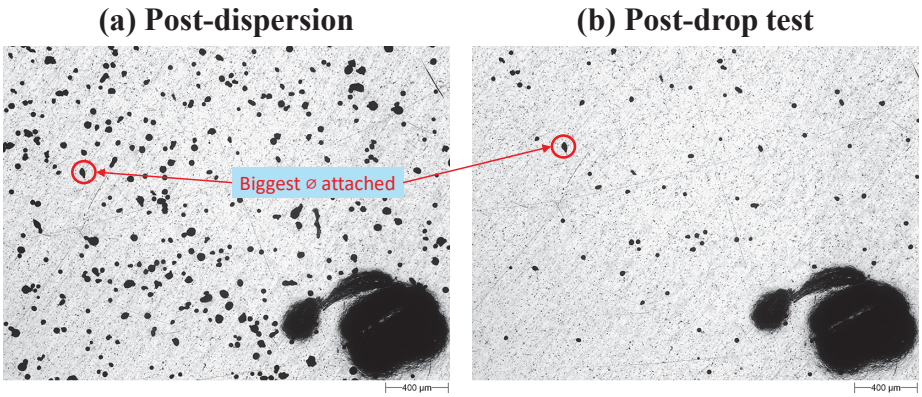

Fig. 15 Al-F particle distribution **(a)** before and **(b)** after the drop test. The black marked area in the bottom right corner of the picture is a reference point. Images are produced by the authors.

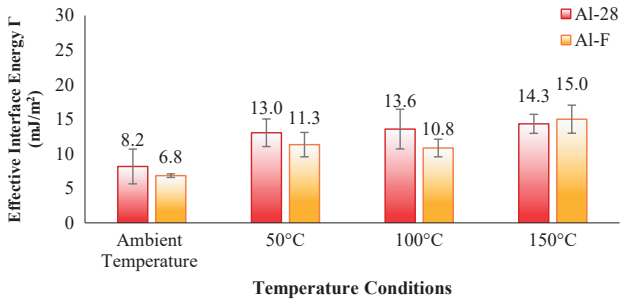

Fig. 16 The effective interface energy (mJ/m^2) of Al-F and Al-28.

was measured in the range of 81.4 and 84.9 µs. For elevated temperature testing, the stubs were placed in an oven at different temperatures (50 °C, 100 °C, and 150 °C) for at least 30 min before being promptly subjected to drop testing. After the drop, the particles were analysed again using the Morphologi G3 to determine the critical particle size of the detached particles (**Fig. 15**). To further elaborate, **Fig. 15(a)** illustrates the post-dispersion image, where a 7 mm^3 of powder was initially dispersed on to the aluminium stub while **Fig. 15(b)** illustrates the post-drop test image, where the particles were subjected to tensile forces after being dropped at a height of 10 cm. By comparing the two captured images, the critical diameter of the particles, above which the particles would detach, can be obtained. The mass of particles with the critical diameter (m) can be used to calculate the interfacial energies between the particles and the aluminium surface based on **Eqn. (2)**.

Fig. 16 shows that for both powders the effective interface energy increased with temperature, leading to greater adhesion forces between the aluminium stub and the particles. This explains the adherence of powders to the funnel surface during the flowrate test at elevated temperatures.

3.8 Spreading characterisation

The in-house spreading rig previously designed at the University of Leeds (Mehrabi et al., 2023) was further developed to characterise the spreading behaviour of powders at elevated bed temperatures, as illustrated in **Fig. 17**. The spreading rig has the capability to produce spread layers, with the flexibility to adjust process parameters such as the spread layer thickness (by adjusting the gap between the blade and the build plate) and spread velocity during experiments, aiming to replicate the real SLM process. A laser profiler with 2-micron resolution (scan CONTROL 2960-25, Micro-Epsilon) was used to measure the height of the powder layer after spreading.

This experiment did not involve the spreading of multiple layers, and the powder layer did not undergo sintering or consolidation to form subsequent layers. Two types of beds made of stainless steel were designed to simulate the build plate during the spreading of powder within the build chamber: a flat bed and one with a rectangular pocket of known dimensions in the middle. The flat bed allows free movement of powders in all directions and resembles spreading under more or less unconfined conditions. The pocket bed simulates spreading of powder under more restricted conditions. Both the flat and pocket beds are equipped with a heating element and a controller that can heat the entire length of the bed up to 700 °C. Heaps of powder were placed on a heated bed in front of a blade (**Fig. 17c**), and their temperature was measured using an infrared thermometer. The spreading test was initiated once the powder bed temperature reached equilibrium.

To analyse the spreading behaviour of both powders at different temperatures (ambient, 50 °C, 100 °C, and 150 °C), a flat bed with a 100-micron gap and a blade speed of 100 mm/s was used, similar to the parameters of the real SLM process (Machno et al., 2022; Oropeza et al., 2022). For analysing the packing index on the flat bed, the spread layer has been analysed to measure the spread area using the open-source ImageJ software. The depth of the spread layer was measured using a laser profiler, while the weight of the spread layer was measured using an analytical balance. The bulk density of the spread layer was then calculated and used to calculate the packing index as follows:

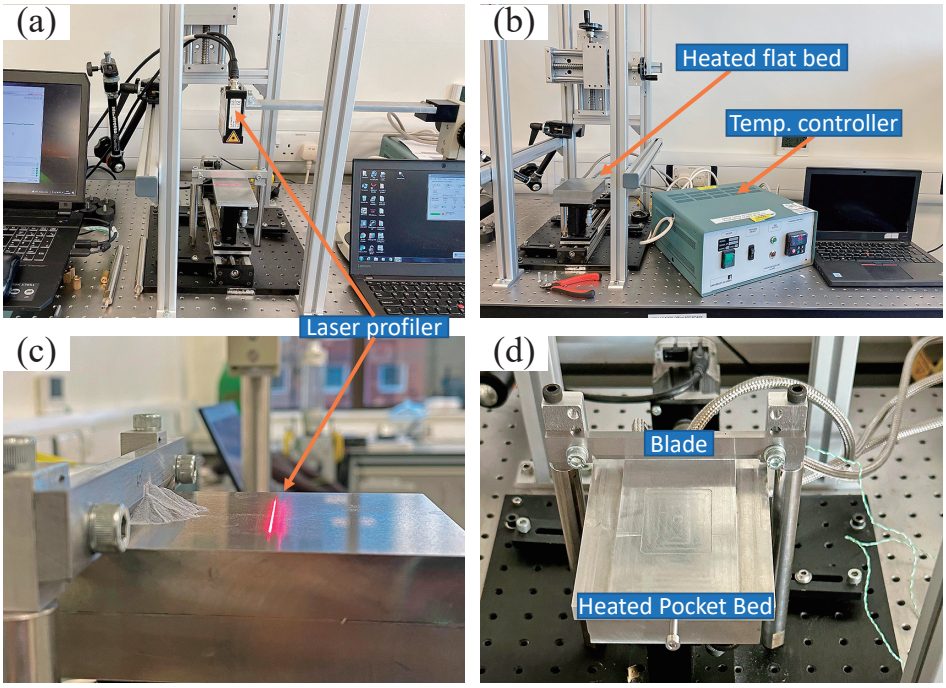

Fig. 17 **(a)** The spreading rig designed and developed at the University of Leeds **(b)** heated bed development **(c)** using laser profiler for the measurement of powder height **(d)** heated pocket bed. Photographs are taken by the authors.

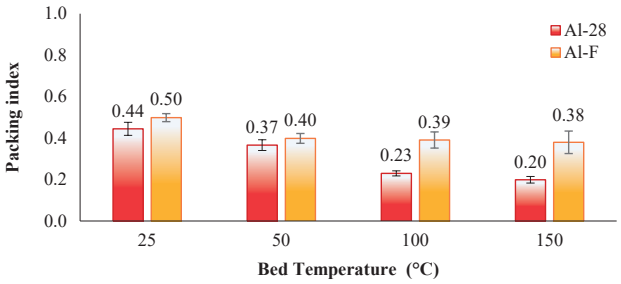

Fig. 18 Spreadability of both powders on heated flat bed, in terms of packing index.

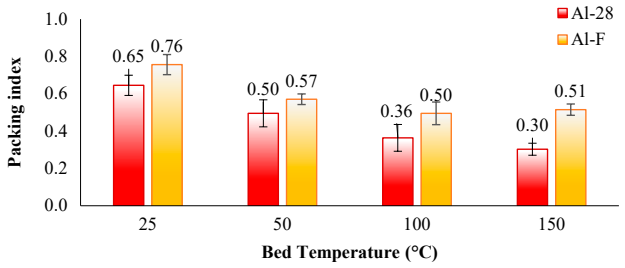

Fig. 19 Spreadability of both powders on pocket bed (100 µm depth), in terms of packing index.

$$Packing\ index = \frac{Bulk\ density\ of\ the\ spread\ layer}{Initial\ bulk\ density\ of\ the\ powder} \quad (3)$$

As shown in **Fig. 18**, at ambient temperature (25 °C), on a flat surface Al-F exhibits better spreadability than Al-28 powder. Al-28 powder with a lower aspect ratio (indicating less spherical particles) leads to looser rearrangement during spreading, resulting in a lower packing index. Both powders exhibited a decline in spreadability with increasing bed temperature, with Al-28 exhibiting a much more significant reduction in packing index.

The spreadability analysis for the pocket bed experiments began with lowering the blade to nearly touch the bed, allowing powder to be deposited only inside the 100 µm-deep pocket. After spreading, the powder inside the pocket was collected and weighed. The bulk density of the powder inside the pocket was then calculated and used in the packing index equation (**Eqn. (3)**).

Fig. 19 shows the packing index of both grades of AlSi10Mg powder after spreading using the pocket bed system (100 µm-depth). While Al-28 powder exhibited a lower packing index on the pocket bed compared to Al-F powder, the overall packing index of both powders for the pocket bed experiments was higher than that under the same conditions on a flat bed. This indicates that powder packing is higher under confined conditions than at the free surface because confinement restricts the movement of free-flowing particles, forcing them to occupy the available space more efficiently. In contrast, on a free surface, free-flowing powders have more freedom to move and settle in a less organised manner.

Furthermore, as observed in the flat-bed experiments, increasing the bed temperature reduced the packing index of the two powders. Again, the reduction in the packing index for Al-28 was more than 50 % from ambient temperature to 150 °C, highlighting the significant impact of bed temperature on the spreadability of this powder.

Overall, it can be seen that the Al-F powder exhibits

better spreadability than the Al-28 powder, which is consistent with the flow behaviour achieved from all the techniques, except the AOR test. This difference may be due to the effect of the particle shape of Al-28 powder, as less spherical particles or particles with more satellites are expected to have a higher tendency to interlock. However, the spreadability of both powders decreased significantly as the bed temperature increased. The reduction in the spreadability can be correlated with the decrease in the powder flow, as obtained from the Carney and Hall flow tests, and stronger powder adherence to the surfaces, as was concluded from the drop test results.

4. Conclusions

The purpose of this study was to investigate the effect of temperature on the bulk flow and spread properties of two different grades of AlSi10Mg metal powders, Al-F and AL-28. Experimental characterisation of the spreading behaviour of these powders at elevated bed temperatures was conducted using an in-house spreading rig, with the aim of developing an understanding of powder behaviour under PBF process-relevant conditions. The results are summarised below:

- As part of this investigation, the flow characteristics of both powders were assessed through various methods, including angle of repose measurements, and assessments of powder compressibility using the Hausner ratio and Carr index. Additionally, flow measurements were conducted using Hall and Carney flowmeters, along with rheological analysis using an FT4 rheometer. Furthermore, the ring shear cell test was conducted to evaluate the shear strength of both powders for a range of consolidation loads. Results from all techniques consistently categorised both powders as free-flowing, with the Al-F powder demonstrating slightly better flowability than the Al-28 powder.
- Among the three different techniques (AOR, shear test and flowrate test) used to analyse the flow behaviour of powder at elevated temperatures, the flowrate test was able to effectively demonstrate the effect of temperature on flowability. The angle of repose did not differ between different temperatures, presumably because the powder cooled down due to the aeration during cone formation. Additionally, the flow properties of the powders from the shear test could not be determined due to the severe stick-slip behaviour of the powder. However, both flowrate methods (Hall and Carney) clearly showed a decrease in powder flowrate with increasing temperature. The tests also suggested an increase in particle adhesion with temperature, as the particles adhered to the funnel at 150 °C.
- The drop test technique was utilised for the first time to measure the surface adhesion of metal powders at ambient and elevated temperatures. The results suggest that as the temperature increases, the effective interfacial energy of both powders increases.
- The packing index for both powders on both flat and pocket beds during spreading test significantly decreased at higher temperatures, possibly attributed to increased interface energy, which was examined and confirmed using the drop test technique.

Acknowledgments

The financial support from EPSRC-UK Future Manufacturing Hub (grant reference: EP/P006566/1, www.mapp.ac.uk), University of Leeds Impact Acceleration Account (grant reference: EP/X52573X/1), and EPSRC-UK Powders by design for additive manufacture through multi-scale simulations (EP/T009128/2) are acknowledged.

We would also like to express our gratitude to Andrew Stockdale and Matthew Buckley for their valuable contributions to the design and development of the heated bed spreading rig.

References

Ajabshir S.Z., Hare C., Sofia D., Barletta D., Poletto M., Investigating the effect of temperature on powder spreading behaviour in powder bed fusion additive manufacturing process by Discrete Element Method, Powder Technology, 436 (2024) 119468. https://doi.org/10.1016/j.powtec.2024.119468

ASTM 52900-15, Standard terminology for additive manufacturing—general principles—terminology, ASTM International, West Conshohocken, PA, 3 (2015) 5. https://doi.org/10.1520/ISOASTM52900-15

ASTM B213-20, Standard test methods for flow rate of metal powders using the hall flowmeter funnel, ASTM International, (2020). https://doi.org/10.1520/B0213-20

Avrampos P., Vosniakos G.-C., A review of powder deposition in additive manufacturing by powder bed fusion, Journal of Manufacturing Processes, 74 (2022) 332–352. https://doi.org/10.1016/j.jmapro.2021.12.021

Bagga P., Brisson G., Baldwin A., Davies C.E., Stick-slip behavior of dairy powders: Temperature effects, Powder Technology, 223 (2012) 46–51. https://doi.org/10.1016/j.powtec.2011.05.015

Balbaa M., Ghasemi A., Fereiduni E., Elbestawi M., Jadhav S., Kruth J.-P., Role of powder particle size on laser powder bed fusion processability of AlSi10mg alloy, Additive Manufacturing, 37 (2021) 101630. https://doi.org/10.1016/j.addma.2020.101630

Carr R.L., Evaluating flow properties of solids, Chemical Engineering, 72 (1965) 163–168.

Chen B., Moon S.K., Yao X., Bi G., Shen J., Umeda J., Kondoh K., Comparison study on additive manufacturing (AM) and powder metallurgy (PM) AlSi10Mg alloys, JOM, 70 (2018) 644–649. https://doi.org/10.1007/s11837-018-2793-4

Clayton J., Millington-Smith D., Armstrong B., The application of powder rheology in additive manufacturing, JOM, 67 (2015) 544–548. https://doi.org/10.1007/s11837-015-1293-z

Cordova L., Campos M., Tinga T., Assessment of moisture content and its influence on laser beam melting feedstock, Euro PM2017, (2017) 6pp.

Dowling L., Kennedy J., O'Shaughnessy S., Trimble D., A review of critical repeatability and reproducibility issues in powder bed fusion, Materials & Design, 186 (2020) 108346. https://doi.org/10.1016/j.matdes.2019.108346

Fouda Y.M., Bayly A.E., A DEM study of powder spreading in additive layer manufacturing, Granular Matter, 22 (2020) 10. https://doi.org/10.1007/s10035-019-0971-x

Freeman R., Measuring the flow properties of consolidated, conditioned and aerated powders—a comparative study using a powder rheometer and a rotational shear cell, Powder Technology, 174 (2007) 25–33. https://doi.org/10.1016/j.powtec.2006.10.016

Ganesan V., Rosentrater K., Muthukumarappan K., Flowability and handling characteristics of bulk solids and powders–a review with implications for DDGS, Biosystems Engineering, 101 (2008) 425–435. https://doi.org/10.1016/j.biosystemseng.2008.09.008

Geldart D., Abdullah E., Verlinden A., Characterisation of dry powders, Powder Technology, 190 (2009) 70–74. https://doi.org/10.1016/j.powtec.2008.04.089

Gibson I., Rosen D.W., Stucker B., Khorasani M., Rosen D., Stucker B., Khorasani M., Additive Manufacturing Technologies, Springer, 2021, ISBN: 9783030561260. https://doi.org/10.1007/978-3-030-56127-7

Grainger L., Investigating the effects of multiple re-use of Ti6Al4V powder in additive manufacturing (AM), Renishaw plc, (2016) 1–9.

Greenspan L., Humidity fixed points of binary saturated aqueous solutions, Journal of Research of the National Bureau of Standards Section A, Physics and Chemistry, 81 (1977) 89. https://doi.org/10.6028/jres.081A.011

Grubbs J., Sousa B.C., Cote D., Exploration of the effects of metallic powder handling and storage conditions on flowability and moisture content for additive manufacturing applications, Metals, 12 (2022) 603. https://doi.org/10.3390/met12040603

Hausner H.H., Friction conditions in a mass of metal powder, Polytechnic Inst. of Brooklyn. Univ. of California, Los Angeles, 1967.

Haydari Z., Talebi F., Mehrabi M., Gardy J., Moeni M., Bayly A.E., Hassanpour A., Insights into the assessment of spreadability of stainless steel powders in additive manufacturing, Powder Technology, 439 (2024) 119667. https://doi.org/10.1016/j.powtec.2024.119667

He Y., Hassanpour A., Bayly A.E., Combined effect of particle size and surface cohesiveness on powder spreadability for additive manufacturing, Powder Technology, 392 (2021) 191–203. https://doi.org/10.1016/j.powtec.2021.06.046

Hulme C.N., Mellin P., Marchetti L., Hari V., Uhlirsch M., Strandh E., Saeidi K., Dubiez-Le Goff S., Saleem S., Pettersson V., A practicable and reliable test for metal powder spreadability: Development of test and analysis technique, Progress in Additive Manufacturing, 8 (2023) 505–517. https://doi.org/10.1007/s40964-022-00341-3

Jacob G., Jacob G., Brown C.U., Donmez A., The influence of spreading metal powders with different particle size distributions on the powder bed density in laser-based powder bed fusion processes, US Department of Commerce, National Institute of Standards and Technology, 2018. https://doi.org/10.6028/NIST.AMS.100-17

Jenike A.W., A theory of flow of particulate solids in converging and diverging channels based on a conical yield function, Powder Technology, 50 (1987) 229–236. https://doi.org/10.1016/0032-5910(87)80068-2

LeBrun T., Standardization gaps in powder feedstock characterization and establishing acceptability for reuse in additive manufacturing, JOM, (2024) 1885–188. https://doi.org/10.1007/s11837-024-06385-w

Li C., Liu Z., Fang X., Guo Y., Residual stress in metal additive manufacturing, Procedia CIRP, 71 (2018) 348–353. https://doi.org/10.1016/j.procir.2018.05.039

Liu Q., Danlos Y., Song B., Zhang B., Yin S., Liao H., Effect of high-temperature preheating on the selective laser melting of yttria-stabilized zirconia ceramic, Journal of Materials Processing Technology, 222 (2015) 61–74. https://doi.org/10.1016/j.jmatprotec.2015.02.036

Liu Z., Huang C., Gao C., Liu R., Chen J., Xiao Z., Characterization of Ti6Al4V powders produced by different methods for selective electron beam melting, Journal of Mining and Metallurgy B: Metallurgy, 55 (2019) 121–128. https://doi.org/10.2298/JMMB181025008L

Machno M., Franczyk E., Bogucki R., Matras A., Zębala W., A comparative study on the structure and quality of SLM and cast AISI 316L samples subjected to WEDM processing, Materials, 15 (2022) 701. https://doi.org/10.3390/ma15030701

Mahamood R., Akinlabi E., Effect of powder flow rate on surface finish in laser additive manufacturing process, IOP Conference Series: Materials Science and Engineering, IOP Publishing, 391 (2018) 012005. https://doi.org/10.1088/1757-899X/391/1/012005

Mehrabi M., Analysis of bulk behaviour of particles based on their individual properties, PhD thesis, University of Leeds, (2021). https://etheses.whiterose.ac.uk/29855/

Mehrabi M., Gardy J., Talebi F.A., Farshchi A., Hassanpour A., Bayly A.E., An investigation of the effect of powder flowability on the powder spreading in additive manufacturing, Powder Technology, 413 (2023) 117997. https://doi.org/10.1016/j.powtec.2022.117997

Mindt H., Megahed M., Lavery N., Holmes M., Brown S., Powder bed layer characteristics: The overseen first-order process input, Metallurgical and Materials Transactions A, 47 (2016) 3811–3822. https://doi.org/10.1007/s11661-016-3470-2

Murtaza H.A., Mukhangaliyeva A., Golman B., Perveen A., Talamona D., Quantitative characterization of metal powder morphology, size distribution, and flowability for additive manufacturing, Journal of Materials Engineering and Performance, 33 (2024) 10853–10867. https://doi.org/10.1007/s11665-023-08761-0

Oropeza D., Penny R.W., Gilbert D., Hart A.J., Mechanized spreading of ceramic powder layers for additive manufacturing characterized by transmission X-ray imaging: Influence of powder feedstock and spreading parameters on powder layer density, Powder Technology, 398 (2022) 117053. https://doi.org/10.1016/j.powtec.2021.117053

Papazoglou E.L., Karkalos N.E., Karmiris-Obratański P., Markopoulos A.P., On the modeling and simulation of SLM and SLS for metal and polymer powders: A review, Archives of Computational Methods in Engineering, (2022) 941–973. https://doi.org/10.1007/s11831-021-09601-x

Prashanth K., Scudino S., Eckert J., Defining the tensile properties of Al-12Si parts produced by selective laser melting, Acta Materialia, 126 (2017) 25–35. https://doi.org/10.1016/j.actamat.2016.12.044

Reijonen J., Revuelta A., Metsä-Kortelainen S., Salminen A., Effect of hard and soft re-coater blade on porosity and processability of thin walls and overhangs in laser powder bed fusion additive manufacturing, The International Journal of Advanced Manufacturing Technology, (2023) 2283–2296. https://doi.org/10.1007/s00170-023-12853-5

Riener K., Oswald S., Winkler M., Leichtfried G.J., Influence of storage conditions and reconditioning of AlSi10Mg powder on the quality of parts produced by laser powder bed fusion (LPBF), Additive Manufacturing, 39 (2021) 101896. https://doi.org/10.1016/j.addma.2021.101896

Rüther M., Klippstein S.H., Ponusamy S., Rüther T., Schmid H.-J., Flowability of polymer powders at elevated temperatures for additive manufacturing, Powder Technology, 422 (2023) 118460. https://doi.org/10.1016/j.powtec.2023.118460

Santos Macías J.G., Douillard T., Zhao L., Maire E., Pyka G., Simar A., Influence on microstructure, strength and ductility of build platform temperature during laser powder bed fusion of AlSi10Mg, Acta Materialia, 201 (2020) 231–243. https://doi.org/10.1016/j.actamat.2020.10.001

Schulze D., Time-and velocity-dependent properties of powders effecting slip-stick oscillations, Chemical Engineering & Technology: Industrial Chemistry-Plant Equipment-Process Engineering-Biotechnology, 26 (2003) 1047–1051. https://doi.org/10.1002/ceat.200303112

Shinohara K., Oida M., Golman B., Effect of particle shape on angle of internal friction by triaxial compression test, Powder Technology, 107 (2000) 131–136. https://doi.org/10.1016/S0032-5910(99)00179-5

Snow Z., Martukanitz R., Joshi S., On the development of powder spreadability metrics and feedstock requirements for powder bed fusion additive manufacturing, Additive Manufacturing, 28 (2019) 78–86. https://doi.org/10.1016/j.addma.2019.04.017

Strondl A., Lyckfeldt O., Brodin H.K., Ackelid U., Characterization and control of powder properties for additive manufacturing, JOM, 67 (2015) 549–554. https://doi.org/10.1007/s11837-015-1304-0

Suryawanshi J., Prashanth K., Scudino S., Eckert J., Prakash O., Ramamurty U., Simultaneous enhancements of strength and toughness in an Al-12Si alloy synthesized using selective laser melting, Acta Materialia, 115 (2016) 285–294.

https://doi.org/10.1016/j.actamat.2016.06.009
Touzé S., Rauch M., Hascoët J.-Y., Flowability characterization and enhancement of aluminium powders for additive manufacturing, Additive Manufacturing, 36 (2020) 101462. https://doi.org/10.1016/j.addma.2020.101462
Venturi F., Taylor R., Additive manufacturing in the context of repeatability and reliability, Journal of Materials Engineering and Performance, 32 (2023) 6589–6609. https://doi.org/10.1007/s11665-023-07897-3
Vock S., Klöden B., Kirchner A., Weißgärber T., Kieback B., Powders for powder bed fusion: A review, Progress in Additive Manufacturing, 4 (2019) 383–397. https://doi.org/10.1007/s40964-019-00078-6
Weiss C., Heslenfeld J., Saewe J.K., Bremen S., Häfner C.L., Investigation on the influence of powder humidity in Laser Powder Bed Fusion (LPBF), Procedia CIRP, 111 (2022) 115–120. https://doi.org/10.1016/j.procir.2022.08.102
Zafar U., Hare C., Hassanpour A., Ghadiri M., Drop test: A new method to measure the particle adhesion force, Powder Technology, 264 (2014) 236–241. https://doi.org/10.1016/j.powtec.2014.04.022
Zhang J., Liu P., Powder flowability characterisation at preheating temperature in additive manufacturing, Powder Metallurgy, 66 (2023) 427–435. https://doi.org/10.1080/00325899.2023.2225953
Zinatlou Ajabshir S., Sofia D., Hare C., Barletta D., Poletto M., Experimental characterisation of the spreading of polymeric powders in powder bed fusion additive manufacturing process at changing temperature conditions, Advanced Powder Technology, 35 (2024) 104412. https://doi.org/10.1016/j.apt.2024.104412

Authors' Short Biographies

Dr. Mozhdeh Mehrabi works as a Post-Doctoral Research Associate (PDRA) in Chemical and Process Engineering at the University of Leeds. She obtained her bachelor's degree in mechanical engineering from the University of Manchester and completed her Master's and PhD degrees in Chemical Engineering at the University of Leeds. Dr. Mehrabi is actively engaged in a broad spectrum of powder technology projects, including but not limited to coating, powder flow dynamics, segregation phenomena, mixing processes, and comprehensive powder spreading characterisation for additive manufacturing. Her expertise lies in the development and enhancement of characterisation methods to address challenges in powder material analysis.

Ms. Fatemeh A. Talebi received her Masters by Research degree in Chemical and Processing Engineering at the University of Leeds, where her research focused on the characterisation of spreadability behaviour in additive manufacturing aligned with MAPP. She is currently pursuing her Ph.D. at the University of Leeds, where her research focuses on particle adhesion of powders through further development of the drop test method.

Dr. Nathan Berry is a Research Associate at the University of Edinburgh where he completed his PhD in granular rheological modelling. His research interests span all scales involved in modelling granular materials. This includes inter-particle interactions, simulations of non-spherical particles and rheological constitutive modelling. Additionally, he is actively involved in projects concerning rheometer experiments with granular materials and complex liquids.

Dr. Sorush Khajepor's work experience, education, and interests encompass mechanics, programming, and mathematics. He describes himself as a multidisciplinary researcher, developer, and problem solver. He holds three degrees in mechanics (BSc, MSc, and PhD) with a focus on fluid flows, solids, heat transfer, and thermodynamics. Since the start of his MSc in Computational Fluid Mechanics (CFD), he has been involved in projects where mathematical challenges are common tasks, including partial differential equations, optimization, and stability analysis. As a researcher at the University of Edinburgh, he focused on additive manufacturing. He numerically and experimentally characterized particle flows at different temperatures.

Dr. Sina Haeri is a Senior Lecturer specialising in particle and particle-laden flows at the School of Engineering, University of Edinburgh. With more than 15 years of expertise in modelling particle-laden and granular flows, Dr. Haeri's research primarily addresses challenges in manufacturing and environmental processes. He has published more than 30 papers in top scientific journals and delivered numerous lectures on the simulation and modelling of additive manufacturing processes to international audiences. Dr. Haeri is esteemed within his field for his seminal work on modelling polymeric powder spreading in the Selective Laser Sintering process.

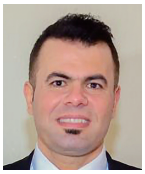

Dr. Jabbar Gardy is a passionate chemist and trained chemical engineer with over 20 years of experience in academia and the pharmaceutical CRO industry, specializing in particle design, material synthesis, powder characterization (both in situ and ex situ), and rig/pilot plant design and installation. He is currently working for Cormica Bradford as a Technical Leader in physical characterisation, where he specializes in delivering analytical solutions, particularly in designing and developing robust methodologies for analysing complex drug development and manufacturing from end to end.

Authors' Short Biographies

Dr. Joseph Oluleke, a chartered engineer and scientist, is the Materials Development Director at Carpenter Additive, having joined the company since 2017. His role, amongst others, involves overseeing the upscaling of the Liverpool powder production plant capacity for special alloy materials like copper, titanium, cobalt, and nickel based super alloys. Prior to this, he worked for four years as the Senior Metallurgist for a leading Oil & Gas R&D company based in the UK. Joseph has contributed, authored, and co-authored several articles for scientific journals within his field of expertise including AM powder post processing, powder behaviour and powder evolution, finite element modelling, microstructural characterisation, mechanical properties testing and corrosion science.

Prof. Andrew Bayly is a chemical engineering expert specializing in particle and droplet behavior to optimize systems and processes. After earning his PhD in multi-phase flow in 1995, he joined Procter & Gamble, where he became a Principal Scientist and an award-winning expert in spray drying. In 2013, he was appointed Chair in Chemical Engineering at the University of Leeds, focusing on processes like spray drying and crystallization. His research spans industries such as food, pharmaceuticals, and fine chemicals, advancing models and techniques to predict process behavior and link it to product structure and properties.

Dr. Ali Hassanpour, is an Associate Professor at the School of Chemical and Process Engineering, University of Leeds. He is fellow of royal society of chemistry and also serves as an executive committee member for Particle Technology Special Interest Group, IChemE. Dr Hassanpour's research has mainly focused on the characterisation of single particle properties and analysis of particles' collective properties and behaviours in different applications, using multi-scale experimental and modelling approaches. He has been involved in numerous research projects at different Technology Readiness Levels, funded by the UKRI, EU and industries. He has published more than 150 archival journal papers, authored 10 book chapters and edited a book on powder flow.